Lasers in Manufacturing Conference 2017

# Influence of dual beam on process stability in laser beam welding of high strength aluminum alloy AA 7075

M. Holzer[a,*], K. Zapf[a], S. Kronberger[a], F. Henkelmann[a], V. Mann[a], K. Hofmann[a], S. Roth[a,c], M. Schmidt[a,b,c]

[a] *Bayerisches Laserzentrum GmbH (blz), Konrad-Zuse-Straße 2-6, 91052 Erlangen, Germany*
[b] *Institute of Photonic Technologies (LPT), Friedrich-Alexander-Universität Erlangen-Nürnberg, Konrad-Zuse-Straße 3-5, 91052 Erlangen, Germany*
[c] *Erlangen Graduate School in Advanced Optical Technologies (SAOT), Paul Gordan Straße 6, 91052 Erlangen*

**Abstract**

Lightweight applications in automotive industries require a steady enhancement due to $CO_2$ emissions and thus light weigth materials have to be applied. So, weldability of high strength aluminum alloy AA 7075 needs to be improved. However, due to its alloying elements magnesium, zinc and copper with high solidification interval and low vaporization temperature, the weldability is limited by hot cracking and keyhole instabilities lead to spatter formation. This paper shows that by using dual beam in laser beam welding, the keyhole can be laterally enlarged and therefore stabilized. Moreover, the energy input can be changed in order to decrease temperature gradient during solidification which leads to a reduction of hot cracking. By applying different beam orientations and distances of dual beam, an improvement of process stability and enhanced solidification conditions could be reached. Process stability is investigated by implementing high speed imaging; hot cracking susceptibility is determined by metallographic inspections. In addition, mechanical characterization shows an increase of weld seam quality and strength.

Keywords: Laser beam welding, dual beam, high strength aluminum, AA 7075, hot cracking

* Corresponding author. Tel.: +49 (0)9131 97790-25; fax: +49 (0)9131 97790-11.
*E-mail address:* m.holzer@blz.org.

## 1. Introduction

Automotive industry needs to applicate improved lightweight constructions in order to increase the performance features of cars regarding low weight. The use of high strength materials is therefore obvious and hence aluminum alloys are already well-established in car body manufacturing. However, due to its low weldability, alloys from series 7xxx e.g. AA 7075 are not in use although they have roughly doubled strength compared to commonly used alloys like AA 5083 or AA 6082. Because of the alloying elements zinc and magnesium with lower evaporation temperatures ($T_{vZn}$ = 907°C; $T_{VMg}$ = 1110°C) compared to aluminum ($T_{VAl}$ = 2470°C) excessive vapor pressure during welding occurs which leads to instability of the keyhole and spatter formation Rapp 1996. Moreover, the contents of copper, magnesium and silicon causes hot cracking during welding of alloys from series 7xxx (Schulze 2010). Investigations regarding the improvement of keyhole stability have been carried out by different research groups. In general keyhole welding of aluminum tends to be more instable because of its low viscosity and low surface tension compared to steel.

Detailed analyses by high speed x-ray analysis of the origin mechanism of process pores and melt ejections can be found in Hohenberger 2003. It was shown that process pores rise if the keyholes back collapses near its bottom which results in a gas inclusion in the melt pool which freezes during solidification. Similar to that melt ejections can be explained; due to a destabilized keyholes back near the top the capillary collapses at surface and due to massive rise of vapor pressure with vaporization of the melt bridge, a large part of the melt pool is ejected. Both defects can be avoided if the keyholes back is continuously stabilized.

In Weberpals 2010 it is shown that by reducing focus diameter from 600 µm to 200 µm and constant divergence angle the geometry of capillary can be influenced which stabilize the keyholes back. This investigation shows an improvement in respect to porosity. It is argued that due to low divergence angle and small focus diameter, the keyhole becomes u-shaped and the total melt volume decreases both leading to a more stable process. A low melt volume results in low turbulences in the melt pool and hence in a reduction of instability. Weberpals 2010 shows that increased process stability by small melt volume can also be reached by increasing the welding velocity which means lower energy per unit length if penetration depth should be constant. Additionally the capillary is widened in welding direction which stabilizes the keyholes back.

A well-known method to stabilize the process in laser beam welding is the dual beam technique. Rapp 1996 includes investigations of dual beam with $CO_2$-Laser and aluminum alloys. By applying both beams in longitudinal direction, porosity and spatter formation could be reduced. Hohenberger 2003 used a dual beam of 300 µm focus diameter and reached lowest porosity in weld seams with both orientations, longitudinal and transverse, by implementing a focus distance of 0.6 mm for welding AA 5052. According to this work, the distance has to be adapted to a maximum where just one capillary is formed. If two separate capillaries occur, process stability decreases and porosity increases again. Those findings could be confirmed by Gref 2005 and transferred to an alloy of 6xxx group. The dual beam welding was also investigated in Haboudou et al. 2003, wherein no influence of the dual beam to HAZ or element loss occurred.

Besides the mentioned dual beam technique some investigations are published in which two different laser beam sources are used for welding. Bielenin et al. used a superimposed diode laser with solid state laser in order to reduce hot cracking in welds of 5xxx und 6xxx alloys. Also Drezet J. -M. et al. 2008 shows results regarding a combination of a solid state laser and a $CO_2$ laser wherein the pulsed solid state laser beam was used to influence solidification by decreasing temperature gradient about factor three. As a result hot cracking could be avoided in welds of AA 6016.

All mentioned investigations deal with aluminum alloys from 5xxx and 6xxx groups. Regarding dual beam welding of aluminum alloys from 7xxx group no work is available jet. Hence it is not clear if the dual beam technique is capable for welding of aluminum alloy with high content of volatile elements Zn and Mg like AA 7075.

## 2. Experimental

### *2.1. Welding setup and process analysis*

All experiments were performed with a continuous wave disc laser, emitting a wavelength of 1,030 nm and a maximal output power of 4 kW. The dual beam was generated by an optic splitting the collimated beam in two equal beams and enabling an adjustable focus distance and orientation; for experiments distances of $a_f$ = 0.3 and $a_f$ = 0.51 mm in combination with longitudinal and vertical orientation according to Fig. 1 were used. The optic and gas nozzle was handled by a 6-axis robot while the clamping device was kept stationary.

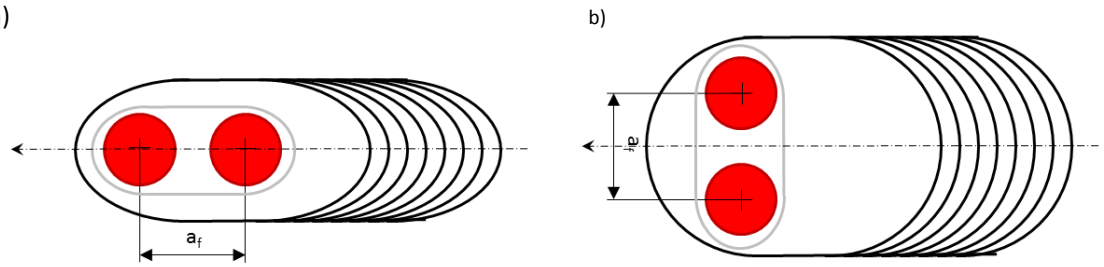


Fig. 1. Schematic drawing of dual beam with distance ($a_f$), keyhole, melt pool and weld seam in a) longitudinal and b) vertical orientation

The used clamping device made of copper (see Fig. 2) ensures a reproducible position of all specimens (1) in butt joint and provides a clamping perpendicular (2) to sheet surface plains. Additionally, clamping in horizontal (3, 4) position is provided in order to prevent slip of specimens due to thermal expansion. All welds were performed with shielding gas Ar 4.6 with mass flow of 25 l/min from top side delivered by leading gas nozzle and 10 l/min from root side (5) of the weld.

1: Specimens in butt joint
2: Vertical clamping
3: Horizontal clamping
4: Screw for horizontal clamping
5: Channel for shielding gas at root side

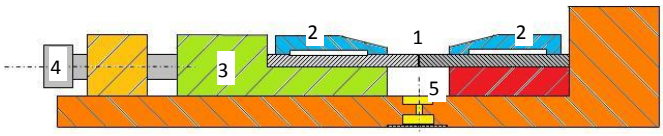


Fig. 2. Schematic drawing of the used clamping device for welding of specimens (1) with vertical (2) and horizontal (3) fixture, screw (4) and channel for shielding gas at root side (5)

The used samples with dimensions of 150 mm x 50 mm x 2 mm were milled and cleaned with isopropanol at joining edge before welding. The rolling direction was parallel to welding direction and edge of 150 mm

length. Aiming a full penetration weld, laser power was set to values, which enable smooth surface of weld seam and root for different welding velocities and the currently used setup of dual beam parameters.

For high speed imaging, a high speed camera system in combination with a pulsed illumination laser with a wavelength of 808 nm and adequate bandwidth filter was used. Camera frequency was set to 37,000 frames per second, while observation angle was about 45° relative to specimen surface and 10° to welding direction for observing the keyhole and surrounding melt.

### *2.2. Chemical analysis and mechanic characterization*

Procedure of metallographic preparation for carrying out the relative hot crack length (RHCL) similar to Holzer et al. 2016 is shown schematically in Figure 3a). Herein for each parameter setup in total one cross section (CS) as well as one longitudinal cross section (LCS), one surface grinding on top (SGt) and bottom (SGb) were prepared for a weld seam length of 20 mm respectively and gauged by light microscopy. Therefore, all samples were grinded and polished to 1 µm graining and etched with NaOH accordingly. An example of a hot crack, detected in a surface grinding, shows Figure 3c; a magnification with measured hot crack length is shown in Figure 3b.

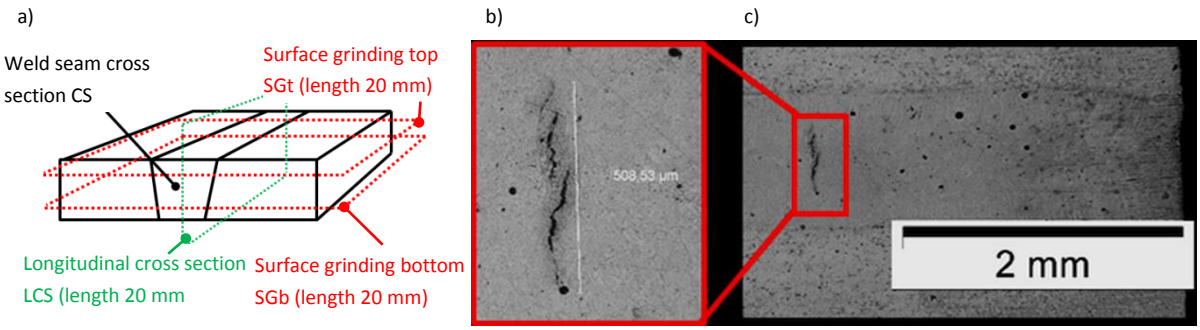


Fig. 3. (a) Schematic drawing of metallographic preparation in cross section (CS), longitudinal cross section (LCS) surface grinding on top (SCt) and bottom (SGb); (b) magnified hot crack with measured length in c) an exemplary surface grinding on top side (SGt)

In order to determine RHCL, the lengths of single cracks ($L_x$) were summed up for all sections according to Equation *(1)*. For determination of a relative hot crack length without dimension, the accumulated length is divided to the analyzed weld seam length of 20 mm.

$$\mathrm{RHCL} = \frac{\sum \mathrm{L_{CS}} + \sum \mathrm{L_{LCS}} + \sum \mathrm{L_{SGt}} + \sum \mathrm{FS_{SGb}}}{20} \left[\frac{mm}{mm}\right] \qquad (1)$$

For the analysis of ultimate tensile strength perpendicular to weld seam, welded samples were cut by laser beam and milled in order to remove thermally influenced material. The specimen geometry is according to standard (DIN 50125) shape “H”. Tensile tests were performed on a tensile tester with continuous test velocity of 5 mm/min. Samples with tempering were first solution annealed during 30 min at a temperature of 480 °C and quenched in water, afterwards age hardened to T6 during 24 h at 125 °C and quenched in water.

## 3. Results and discussion

### *3.1. Process stability*

The process analysis by high speed imaging shows maximal length and width of keyhole, which was determined in order to evaluate the stability of keyhole and to compare this data with weld seam width. Hence, effects regarding keyhole collapse and weld seam quality (next section) can be explained. Fig. 4a) and b) show that maximal and largest minimal keyhole length occur in all cases of 0.51 mm distance and longitudinal orientation of dual beam naturally. Excepting for welding speed of 2 m/min, no significant change in maximal keyhole length can be detected in the parameter field. Compared to minimal keyhole length in Fig. 4b), similar findings can be seen. Minimal keyhole length shows the highest deviation for welding speed of 6 m/min. Length of keyhole varies roughly in the range of 0.5 mm to 1 mm.

a) b)

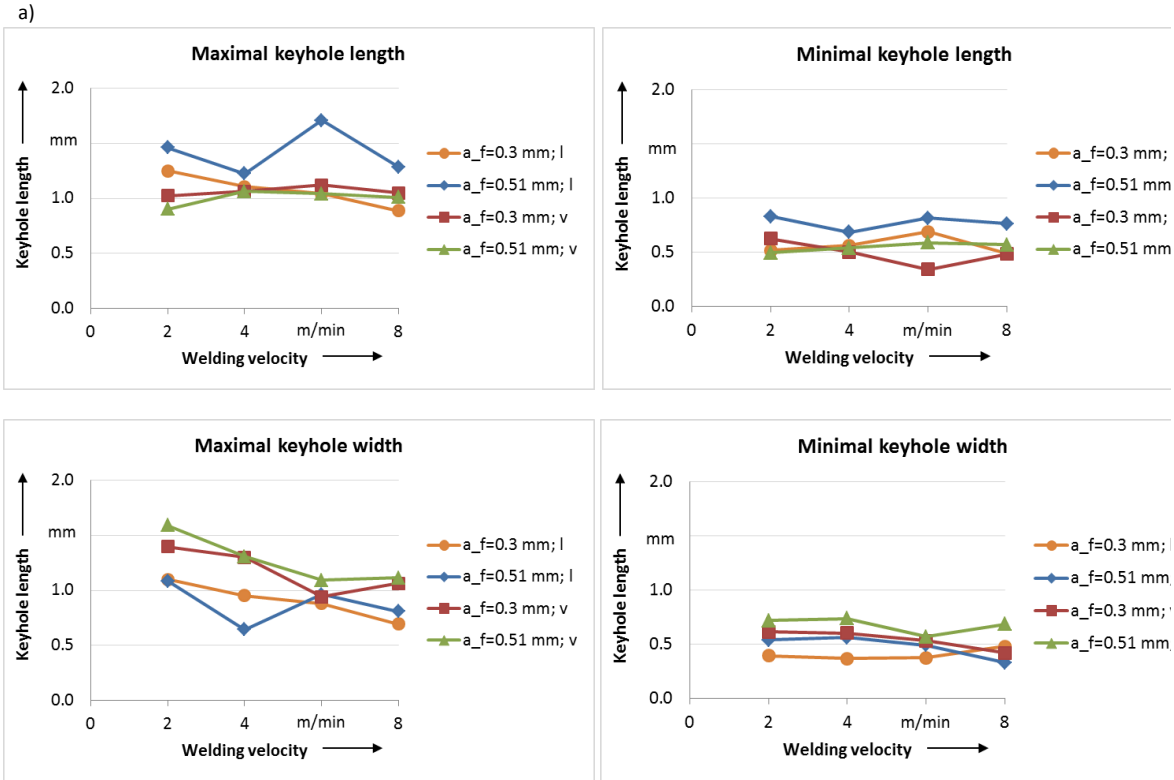


c) d)

Fig. 4. Geometrical determination of a) maximal and b) minimal keyhole length and c) maximal and d) minimal keyhole width; dual beam at 2 mm sheets of AA 7075; with different distances of foci of 0.3 mm and 0.51 mm (a_f) and orientations (l: longitudinal and v: vertical)

Owed to an increase of welding velocity, the maximal keyhole width generally decreases in Fig. 4c). Due to the vertical orientation of beams, the resulting widths show maximal values. Similar to minimal length, the

minimal keyhole width is nearly constant for all welding velocities. In Fig. 5a) the weld seam width is plotted which is shown in relation to maximal keyhole width in Fig. 5b). This information gives conclusions to melt pool flow.

a) b)

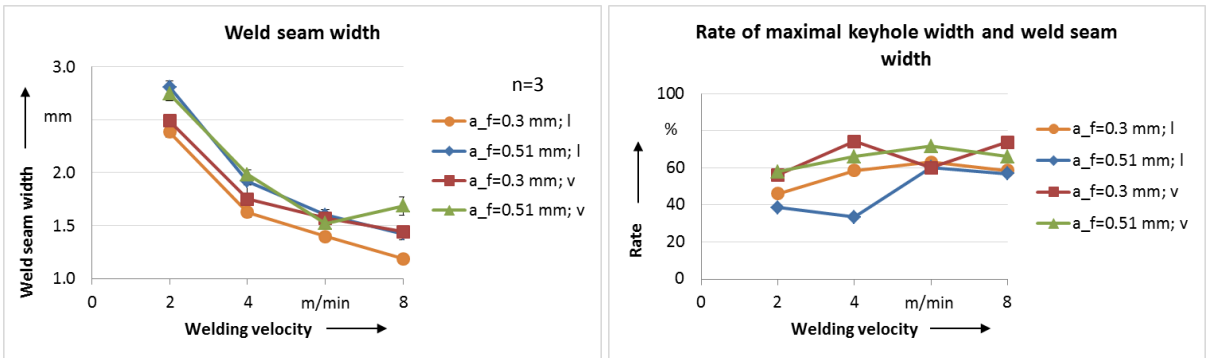


Fig. 5. a) Weld seam width (n=3) and b) rate of maximal keyhole width and weld seam width; dual beam at 2 mm sheets of AA 7075; with different distances of foci of 0.3 mm and 0.51 mm (a_f) and orientations (l: longitudinal and v: vertical)

If the rate of keyhole width to melt pool width increases, high velocities in melt pool are proposed in Weberpals 2010 which leads to destabilize the keyholes back and therefore its total stability. Hence, Fig. 5b) shows an increase of rate with increasing welding velocity. By analyzing the process with high speed imaging, the number of keyhole collapses were detected, which indicates the amount of spatter since every collapse leads to spatter formation (Holzer et al. 2015). This information can be related either to weld seam length or to welding time. As Fig. 6a) shows, the number of collapses per weld seam length decreases with increasing welding velocity for longitudinal beam orientation and is nearly constant for vertical beam orientation. The number of collapses per second in Fig. 6b), however, shows in tendency an increase with increasing welding velocity. This is in good agreement to Weberpals 2010.

a) b)

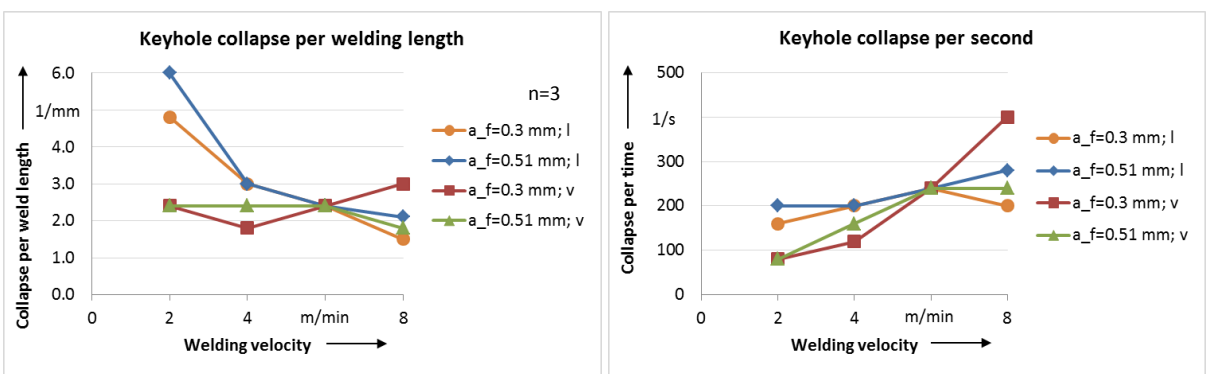


Fig. 6. Number of keyhole collapses per a) weld seam length and b) per second; determined in 25 ms sequence of high speed imaging of weld seams; welded with 200 µm diameter dual beam at 2 mm sheets of AA 7075; with different distances of foci of 0.3 mm and 0.51 mm (a_f) and orientations (l: longitudinal and v: vertical)

According to Klein et al. 1996 regarding general oscillation theory and Holzer et al. 2015 regarding keyhole collapses in pulsed laser beam welding of AA 7075, the Eigenfrequency of keyhole and subsequently the frequency of collapse decreases with increasing volume of melt. An increase of melt volume results, if focus distance is changed from 0.3 mm to 0.51 mm and if welding velocity is decreased (see Fig. **5**a). In order to determine the influence of dual beam configuration on process stability, the weld seam width must be compared to the number of collapses per weld seam length. The results show a significant influence of the beam orientation to keyhole stability when welding with 2 m/min. High speed imaging show that configurations with beam distance of 0.51 mm partially lead to a separation of the keyhole with generation of two keyholes. This leads to instabilities which is also stated in Hohenberger 2003. In order to achieve high weld seam quality, number of keyhole collapse per welding length should be minimized; hence, from this point of view high welding velocities can be recommended.

### *3.2. Weld seam quality*

For determination of the influence of dual beam on process stability and subsequently weld seam quality, samples welded with single beam out of former work Holzer et al. 2016 are shown in comparison. Unfortunately for single beam welding no results with a welding velocity of 8 m/min exist, but welds with velocity of 10 m/min. The following results in Fig. **7** to Fig. **10** show top views and cross sections of welds produced with dual beam - besides references welded with single beam - in four different configurations regarding Fig. **1** with $a_f$ = 0.3 mm and $a_f$ = 0.51 mm combined with longitudinal and vertical orientation. For all four configurations welding velocity was set to $v_l$ = 8 m/min, $v_l$ = 6 m/min, $v_l$ = 4 m/min and $v_l$ = 2 m/min and laser power was adapted to reach a proper weld surface and root. Fig. **7** includes from a) to d) top views of welds performed with welding velocity of 8 m/min. Similar to results generated with single beam, fluctuations of texture in weld seam surface occur, however, it appears more homogenous due to a more stable process. Weld seams slightly differ due to welding parameters and dual beam configuration in width.

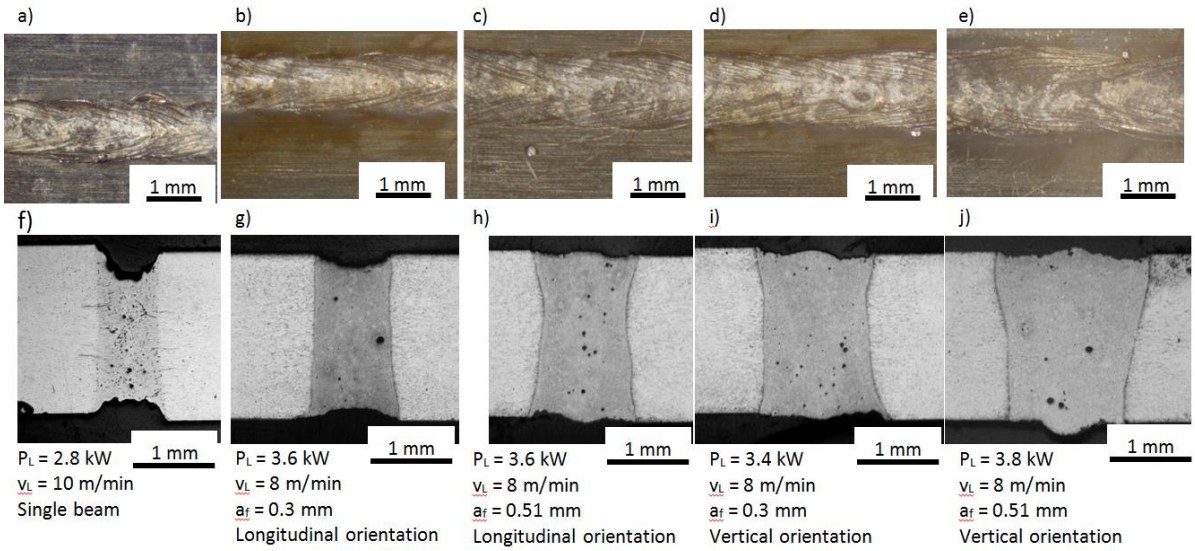


Fig. 7. Weld seams welded with 200 µm diameter dual beam at 2 mm sheets of AA 7075; a) reference with single beam; b) to d): top view of weld seams with welding velocity of 8 m/min (10 m/min single beam) and with different distances of foci of 0.3 mm and 0.51 mm ($a_f$) and orientations; f) to j) cross sections according to top views

A comparison of weld seam cross sections clarifies the influence of dual beam configuration more detailed. A longitudinal orientation and distance of 0.3 mm results in parallel seam shape, whereas an increase in focus distance to 0.51 mm h) leads to x-shaped cross section. A vertical orientation results in higher weld seam width i) due to adapted temperature field; an increased beam distance j) leads to a slight change of shape from parallel to v-shaped. Due to larger beam distance, rate of heat loss due to heat conduction is increased; hence, more laser power is necessary in order to gain a proper weld seam. This higher amount of heat dissipation is considered to lead to the shown x- or v-shape of cross sections.

Fig. **8** shows in sections b) to e) top views of welds performed with welding velocity of 6 m/min. Similar to results generated with single beam shown in a), fluctuations of texture in weld seam surface occur, however, it appears more uniform. Cross section shapes appear in analogy to cross section shapes in Fig. **7**). However, notches at top and root side of configuration with vertical beam orientation and 0.3 mm beam distance (Fig. **8**i) appear. The irregular shape in Fig. **8**j) is a consequence of process instability which leads to loss of volume and poor quality of weld.

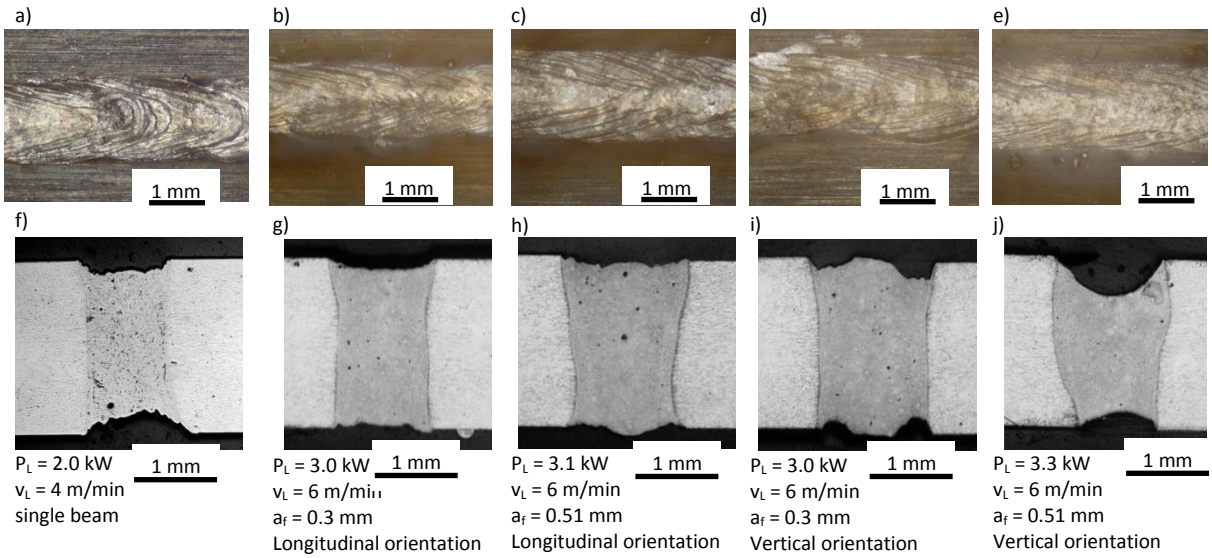


Fig. 8. Weld seams welded with 200 µm diameter dual beam at 2 mm sheets of AA 7075; a) reference with single beam; b) to d): top view of weld seams with welding velocity of 6 m/min and with different distances of foci of 0.3 mm and 0.51 mm ($a_f$) and orientations; f) to j) cross sections according to top views

**Fig. 9** shows in sections b) to e) top views of welds performed with welding velocity of 4 m/min. Similar to results generated with single beam shown in a), fluctuations of texture in weld seam surface occur, however, it appears more uniform. Cross sections width differs due to dual beam distance and orientation. Cross sections show in every configuration loss of volume which is a hint to spatter formation or melt ejections.

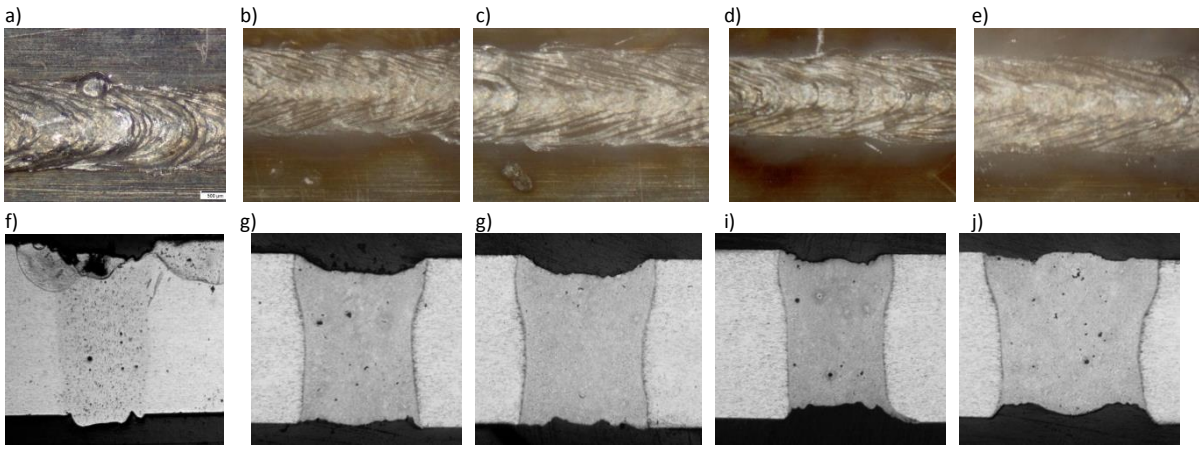


Fig. 9. Weld seams welded with 200 µm diameter dual beam at 2 mm sheets of AA 7075; a) reference with single beam; b) to d): top view of weld seams with welding velocity of 4 m/min and with different distances of foci of 0.3 mm and 0.51 mm ($a_f$) and orientations; f) to j) cross sections according to top views

Fig. **10** shows in sections b) to e) top views of welds performed with welding velocity of 2 m/min. Similar to results generated with single beam shown in a), fluctuations of texture in weld seam surface occur, however, it appears more uniform. Cross sections width differs due to dual beam distance and orientation. Cross sections show in every configuration in comparison to 4 m/min welding velocity lower loss of volume.

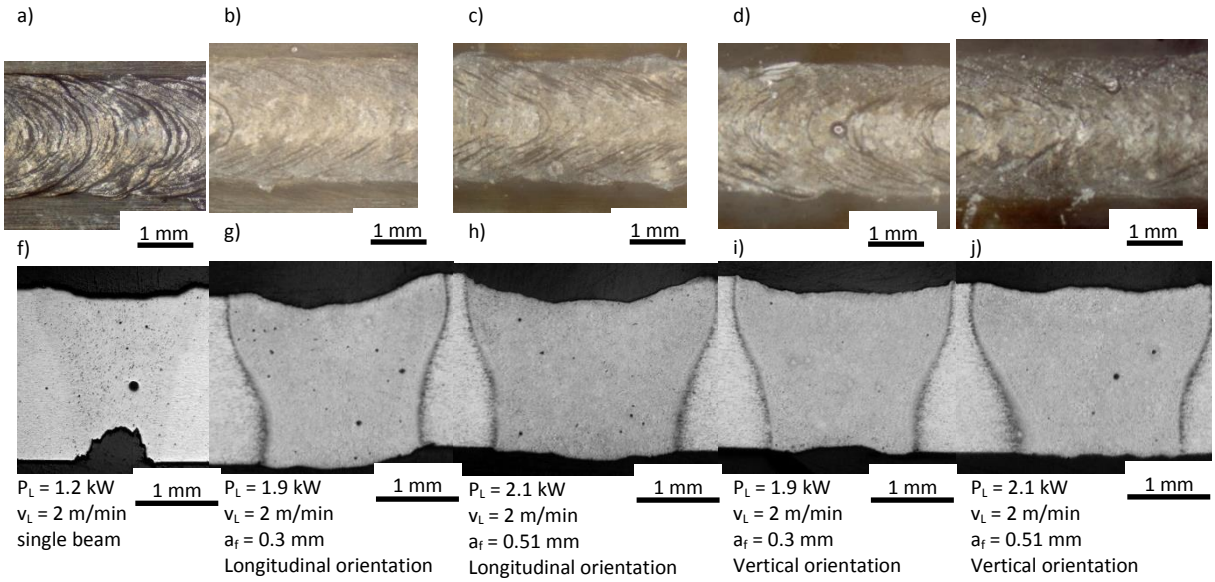


Fig. 10. Weld seams welded with 200 µm diameter dual beam at 2 mm sheets of AA 7075; a) reference with single beam; b) to d): top view of weld seams with welding velocity of 2 m/min and with different distances of foci of 0.3 mm and 0.51 mm ($a_f$) and orientations; f) to j) cross sections according to top views

Cross sections welded with dual beam in comparison to weld seams welded with single beam show higher quality by means of irregularities at weld seam surface and cross sections. Dual beam leads to an enlargement of the keyhole following the orientation of beams, which enables an enhanced outgassing of the high vapor rate by contents of Mg and Zn. Additionally, the larger melt pools and therefore the lower rate of maximal keyhole width and weld seam width reduce melt pool flow and hence minders the destabilization of the keyholes back Weberpals 2010. In tendency, this effect increases with decreasing welding velocity (see Fig. **5**b).

### *3.3. Mechanical properties*

Mechanical properties are highly dependent on weld seam defects like hot cracking or irregularities in cross section. Hence the relative hot crack length (RHCL) was determined and is shown and compared to welds with single beam in Fig. **11**a). It can be seen that a welding velocity of 2 m/min results in no hot cracking, welding velocity of 4 m/min in nearly no hot cracking and welding velocity of 6 m/min and 8 m/min in high hot cracking. Highest RHCL for 6 m/min and 8 m/min show the weld seam produced with vertical orientation and 0.51 mm beam distance followed by remaining welds. In the parameter sets with 8 m/min welding velocity the second highest RHCL show longitudinal orientation with 0.3 mm beam distance. Lowest hot cracking contain welds produced with longitudinal orientation and 0.51 mm beam distance. According to investigations on dual beam for reducing hot cracking in Bielenin et al. and Drezet J. -M. et al. 2008 lower temperature gradients lead to reduced hot cracking which can be reached by implementing high distance of

beams and a longitudinal orientation. The comparison with RHCL of welds with single beam for 8 m/min cannot be drawn because of missing data point.

Mechanical properties are determined by tensile tests with specimen without treatment and with tempering in order to eliminate softening in weld seam and heat affected zone. As Fig. 11b) and c) demonstrate, dual beam configurations show better performance compared to single beam for weld seams welded with 2 m/min. In general, strength of base material (> 540 MPa) could roughly be reached. However due to low standard deviations, no significant effect of dual beam configurations on strength could be determined.

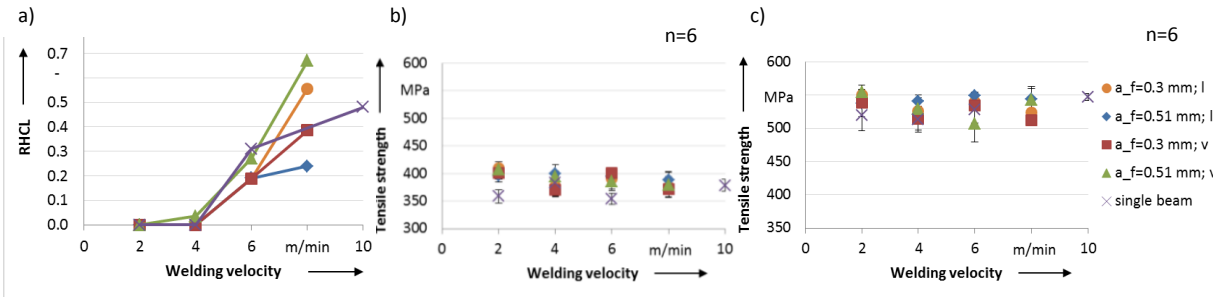


Fig. 11. a) Relative hot crack length(RHCL); b) tensile strength without treatment and c) with heat treatment of samples welded with 200 µm focus diameter dual beam at 2 mm sheets of AA 7075 with different distances of foci of 0.3 mm and 0.51 mm (a_f) and orientations (l: longitudinal and v: vertical)

## 4. Conclusion

The present work shows the possibility to increase weldability of high strength aluminum alloy AA 7075 by using a dual beam with 200 µm focus diameter, focus distances of 0.3 mm and 0.51 mm positioned in vertical and horizontal direction. By implementing high speed camera analysis of the process, keyhole stability by means of its dimensions and number of keyhole collapse per time could be investigated. It was demonstrated, that the dual beam orientation has no significant influence on the number of keyhole collapses while low welding speed of 2 m/min and longitudinal orientation results in lowest process stability regarding keyhole collapses. Top views and cross sections of all welds show higher quality in surface texture of weld seams compared to weld seams produced by single beam. Regarding the shape of cross sections, larger width of weld seam can be reached in general with reduced loss of volume in comparison to single beam. In order to achieve high weld seam quality, number of keyhole collapse per welding length should be minimized; hence, high welding velocities can be recommended.

The influence of dual beam on relative hot crack length was shown. In this case low welding velocity can be recommended, since no hot cracks could be found in welds produced with 2 m/min. Especially with welding velocity of 6 m/min a significant benefit of dual beam on hot cracking could be found. Low hot cracking due to enhanced solidification conditions occur, if a high distance of 0.51 mm in longitudinal orientation is used. An enhancement of tensile strength could be reached in tendency compared to single beam. After heat treatment, samples show tensile strength in range of base material.

## Acknowledgements

The authors gratefully acknowledge funding of the Bavarian Ministry of Economic Affairs and Media, Energy and Technology by the funding program Electric Mobility and the Project Management Bavaria (ITZB).

## References

Bielenin, M.; Bergmann, J. P.; Witzendorff, P. von; Hermsdorf, J. Prozessstrategie zur Stabilisierung des gepulsten Laserstrahlschweißens und zur Verbesserung der Nahtgüte beim Schweißen von Aluminiumwerkstoffen mittels Kombination eines Diodenlasers mit einem gepulsten Festkörperlaser, Schlussbericht zum AiF-Vorhaben 17487 BG.

Drezet J. -M.; Wagniere J. -D.; Rappaz M.; Kurz W.; Lima M. S. F. 2008. Crack-free aluminium alloy welds using a twin laser process. In: Welding in the World 52, S. 87–94, SPEC. ISS.

Gref, W. 2005. Laserstrahlschweißen von Aluminiumwerkstoffen mit der Fokusmatrixtechnik. Dissertation. Universität Stuttgart, Stuttgart. IFSW.

Haboudou, A.; Peyre, P.; Vannes, A. B.; Peix, G. 2003. Reduction of porosity content generated during Nd:YAG laser welding of A356 and AA5083 aluminium alloys. In: Materials Science & Engineering A 363, S. 40–52, 1-2.

Hohenberger, B. 2003. Laserstrahlschweissen mit Nd:YAG-Doppelfokustechnik - Steigerung von Prozessstabilität, Flexibilität und verfügbarer Strahlleistung. Dissertation. Universität Stuttgart, Stuttgart. Institut für Strahlwerkzeuge (IFSW).

Holzer, M.; Hofmann, K.; Mann, V.; Hugger, F.; Roth, S.; Schmidt, M. 2016. Change of Hot Cracking Susceptibility in Welding of High Strength Aluminum Alloy AA 7075. In: PHPRO Physics Procedia 83, S. 463–471.

Holzer, M.; Straub, O.; Hofmann, K.; Hugger, F.; Roth, S. 2015. Influence of pulse shape on crack and spatter formation in laser beam welding of aluminum alloy with high content of zinc. In: Proceedings of LAMP 2015. Japan.

Klein, T.; Vicanek, M.; Simon, G. 1996. Forced oscillations of the keyhole in penetration laser beam welding. In: Journal of Physics D: Applied Physics 29, S. 322–332, 2.

DIN 50125, 2009. Prüfung metallischer Werkstoffe - Zugproben.

Rapp, J. 1996. Laserschweisseignung von Aluminiumwerkstoffen für Anwendungen im Leichtbau. Dissertation. IFSW, Stuttgart.

Schulze, G. 2010. Die Metallurgie des Schweißens, Eisenwerkstoffe - Nichteisenmetallische Werkstoffe. 4. Aufl., Springer, Heidelberg.

Weberpals, J.-P. 2010. Nutzen und Grenzen guter Fokussierbarkeit beim Laserschweissen. Utz, München.